Properties of Human Vasopressin Precursor Constructs: Inefficient Monomer Folding in the Absence of Copeptin as a Potential Contributor to Diabetes Insipidus†

Chandana Barat,§ LeRone Simpson, and Esther Breslow*

Department of Biochemistry, Weill Medical College of Cornell University, 1300 York Avenue, New York, New York 10021

Received January 21, 2004

ABSTRACT: These studies were aimed at an initial characterization of the human vasopressin precursor and the evaluation of factors leading to misfolding by the pathological 87STOP mutation. This mutation deletes the precursor's glycosylated copeptin segment, which has been considered unnecessary for folding, and the last seven neurophysin residues. We investigated the role in folding of the last seven neurophysin residues by comparing the properties of the 87STOP precursor and its derivative neurophysin with those of the corresponding wild-type proteins from which copeptin had been deleted, leading to the following conclusions. First, despite modulating effects on several protein properties, the last seven neurophysin residues do not make a significant net thermodynamic contribution to precursor folding; stabilities of the mutant and wild-type precursors to both guanidine denaturation and redox buffer unfolding are similar, as are in vitro folding rates. Second, the monomeric forms of both precursors are unstable and predicted to fold inefficiently at physiological pH and temperature, as evidenced by precursor behavior in redox buffers and by thermodynamic calculations. Third, both precursors are significantly less stable than the bovine oxytocin precursor. These results, together with earlier studies elsewhere of vasopressin precursor behavior within rat neurons, are shown to represent a self-consistent argument for a role for glycosylated copeptin in vasopressin precursor folding in vivo, copeptin most probably assisting refolding by facilitating interaction of misfolded monomers with the calnexin/calreticulin system. This hypothesis provides an explanation for the absence of copeptin in the more stable oxytocin precursor and suggests that the loss of copeptin contributes to 87STOP pathogenicity. Reported cell culture studies of rat precursor folding are also discussed in this context. Most generally, the results emphasize the significance of monomer stability in the folding pathways of oligomeric proteins.

The role of protein misfolding in disease is increasingly recognized, although mechanisms contributing to misfolding are inadequately understood. The disorder familial neurogenic diabetes insipidus is representative of systems via which these mechanisms can be elucidated. This disorder is associated with the degeneration of vasopressin-secreting neurons and arises from mutations in the human vasopressin (VP)[1] precursor (e.g., refs *1*−*5*). All diabetes insipidus-associated mutants studied thus far show partial or complete retention in the endoplasmic reticulum; this retention is assumed to underlie the cell pathology and to arise from precursor misfolding (e.g., refs *1*−*5*). Figures 1 and 2 show the structure of the VP precursor following excision of its signal sequence in the ER. The structure sequentially consists (*6*) of the sequences of VP, a GKR linker, the protein neurophysin (NP), a linker R residue, and copeptin (CP), a C-terminal glycopeptide of unknown function. Most of the pathological mutations lie within the NP sequence, but pathological mutations in the signal peptide and hormone sequences have also been identified (*4*, *7*). The hormone oxytocin is synthesized via a similar precursor, which contains a highly homologous NP (Figure 1) but which lacks copeptin (*8*).

The mechanisms by which most diabetes insipidus mutations impair folding can be predicted on the basis of what is known about NP properties (e.g., refs *1* and *9*). Moreover, the ability of a number of these mutations to adversely affect NP folding has been experimentally confirmed by studying the effects of their incorporation into the NP component of the bovine oxytocin precursor (*9*). However, the pathogenicity of two mutations is not yet understood. These are the G57S mutation, the effects of which on the bovine oxytocin precursor and its derivative NP are relatively minor (*9*), and the 87STOP mutation. The C-terminal NP residues deleted by the 87STOP mutation are not resolved in ^{VP}BNP crystal

† Supported by Grant GM-17528 from NIH.

* To whom correspondence should be addressed. Department of Biochemistry, Weill Medical College of Cornell University, 1300 York Ave., New York, NY 10021. Tel.: 212-746-6428. Fax: 212-746-8875. E-mail: ebreslow@med.cornell.edu.

§ Present address: Wadsworth Center, N.Y. State Department of Health, P.O. Box 509, Albany, N.Y. 12201-0509.

[1] Abbreviations: VP, vasopressin (in this case arginine vasopressin); NP, neurophysin; CP, copeptin; ^{Oxy}BNP, NP derived from the bovine oxytocin precursor; ^{VP}BNP, NP derived from the bovine VP precursor; HVP, human vasopressin precursor; HVPΔCP, human vasopressin precursor minus copeptin; ^{VP}HNP, NP derived from the human VP precursor; ^{VP}HNP-CP, ^{VP}HNP with copeptin attached; ^{VP}RNP, NP derived from the rat VP precursor; Phe-PheNH_2 or Phe-Phe amide, L-phenylalanyl-L-phenylalanine amide; Phe-TyrNH_2, L-phenylalanyl-L-tyrosine amide.

10.1021/bi0400094 CCC: $27.50
Published on Web 06/02/2004

```
                        10                  20                  30
OxyBNP  A V L D L D V R T C L P C G P G G K G R C F G P S I C C G D E L G C F
VPBNP   ---M S-------E L--- Q ----------------------------------------------
VPHNP   ---M S-------E L----Q----------------------------------------A-------

                40                  50                  60                  70
OxyBNP V G T A E A L R C Q E E N Y L P S P C Q S G Q K P C G S G G R C A A A
VPBNP  ----------------------------------------------------------------------
VPHNP  ----------------------------------------------------A-----------------F

                        80                  90
OxyNP   G I C C  S P D G C H E D P A C D P E  A A F S Q
VPBNP    ----------N D E S ---V T E----E ---R E G IV G---P R R V
VPHNP   --V------ N D E S----V T E---E----R E G--F H[   ]R R A
VPRNP                                      F F [   ]R L T

R[ASDRSNATQLDGPAGALLLRLVQLAGAPEPFEPAQPDAY]

[Human copeptin] with preceding R linker residue
```

FIGURE 1: Amino acid sequences of ^{Oxy}BNP, ^{VP}BNP, and ^{VP}HNP, together with the copeptin sequence of the human VP precursor (HVP) and the C-terminal sequence of ^{VP}RNP. Neurophysin sequences are from ref *27*. The copeptin sequence is from ref *41*.

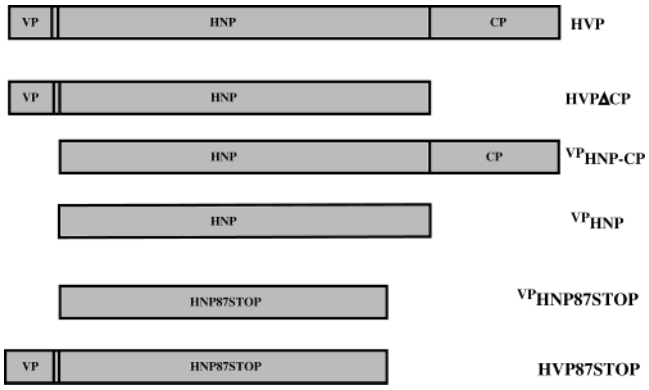

FIGURE 2: Principal expression products investigated. In addition, precursor terminating with NP residue 89 (HVP90STOP) was studied. The sequence Gly-Lys-Arg separates the hormone and NP sequences, and a single Arg residue separates the NP and CP sequences. All expression products are preceded by the sequence Met-His Tag-TrpLE-Met, which is cleaved by CNBr.

structures (e.g., ref *10*), and termination of the sequences of ^{Oxy}BNP and ^{VP}BNP with position 86 was unaccompanied by effects clearly relevant to folding (ref *9* and Discussion). These results suggested that factors unique to the human VP precursor might be involved in the pathogenicity of the G57S and 87STOP mutations (*9*). In subsequent unpublished studies, we examined the effect of the 87STOP mutation on ^{Oxy}BNP that had been mutated to incorporate the unique A70F and P60A substitutions of ^{VP}HNP (Figure 1), but the results were again not illuminating. Accordingly, we investigated the effects of mutation directly on the human VP precursor.

Apart from a study of the self-association properties of semisynthetic bovine VP precursor analogues (*11*), the biophysical properties of VP precursors are unknown and, to our knowledge, no biophysical studies of the human VP precursor, of ^{VP}HNP, or of copeptin have been performed. We report here the synthesis of cDNA encoding the human VP precursor and derivatives thereof, the expression of these proteins in *Escherichia coli*, a survey of their folding and related biophysical properties, and an investigation of the effects of the 87STOP mutation. The expressed proteins typically differ from those of the WT human protein in the substitution of Leu for Met in position 2 of NP (Figure 1**)**

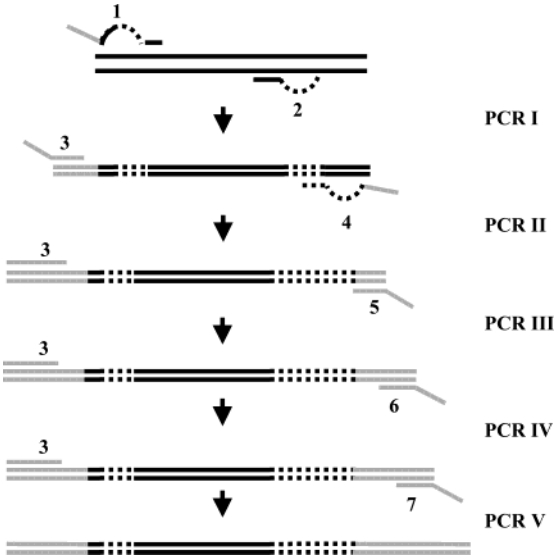

FIGURE 3: Major steps in the conversion of the sequence of the P60A, A70F double mutant of ^{Oxy}BNP to the sequence of HVP by PCR. The sequence differences between the N- and C-terminal domains of ^{Oxy}BNP and ^{VP}HNP (Figure 1), except for the substitution of Met-2 of ^{VP}HNP by Leu (see text) were incorporated by PCR as shown in step I applying a procedure used for PCR-based epitope tagging of proteins (e.g., ref *42*). The cDNA product was then extended by a similar procedure at both ends by sequential incorporation of the vasopressin and CP sequences at the N- and C-termini, respectively (Steps II−V). See Methods for subsequent steps.

and in the lack of glycosylation of the CP segment. Studies of ^{VP}BNP (*12*) and others reported below support the lack of importance of Met in position 2, while removal of the CP glycosylation signal is reported to be without effect on the biological handling of the rat VP precursor in cell culture (*13*). Additionally, CP itself has typically been considered unnecessary for precursor folding (e.g., ref *1*) because of its absence in the closely related oxytocin precursor and because CP deletion appears to actually facilitate processing of the rat VP precursor in cell culture (*14*). Because of the putative lack of contribution of CP to precursor folding, our studies of the 87STOP mutation initially focused on the potential influence on folding of the seven C-terminal NP residues deleted by the mutation. However, the ultimate results are shown to suggest an important role for glycosylated CP in folding and potential reasons for its greater importance to the VP precursor than to the oxytocin precursor.

MATERIALS AND METHODS

Synthesis of cDNA Constructs. Synthesis of the cDNA encoding the bovine oxytocin precursor, its derivative NP, and mutants thereof has been reported earlier (*9*, *15*). The cDNA encoding the P60A, A70F double mutant of ^{Oxy}BNP (Figure 1), was converted to the cDNA of the full-length human VP precursor, albeit with retention of the A29G and V72I substitutions of ^{Oxy}BNP (Figure 1), by N- and C-terminal additions and replacements (Figure 3). This cDNA was cloned into the expression plasmid pTMHa30−51, thus attaching it to a Met-His tag-TrpLE-Met sequence at its amino-terminus (*15*). Finally, the human substitutions at positions 29 and 72 were incorporated (Stratagene Quikchange site directed mutagenesis kit). Note that the Met preceding the precursor sequence allows cleavage of the

expressed precursor from the His tag and TrpLE sequences by CNBr treatment, this treatment necessitating the substitution of Leu for Met-2 of ^{VP}HNP; a full-length precursor construct with Ala in position 2 was also prepared (Results). The cDNA encoding the precursor without CP was prepared by mutating the Arg codon immediately following the NP sequence to a STOP. The clones expressing the NP-CP and NP components alone were obtained by PCR amplification of the full-length or ΔCP precursor cDNA sequences using appropriate primers to delete theVP sequence and then subcloning into the BamH1−Hind111 site of the expression vector. However, in the construction of cDNA encoding NP-CP, the Met in position 2 of NP was inadvertently not substituted, leading to two expression products (vide infra).

The cDNAs encoding the 87STOP precursor and its derivative NP were prepared from those encoding HVP and its derivative NP respectively by mutation of the triplet encoding Glu-87 of NP to a STOP. The cDNA encoding a 90STOP precursor was prepared by analogous mutation of the His-90 triplet. The structures of all constructs were confirmed by sequencing **(**DNA Sequencing Facility, Bioresource Center of Cornell University, Ithaca, NY). Relationships among the major constructs are summarized in Figure 2.

Protein Expression, Folding, and Purification. The His-tagged fusion proteins were expressed in *E. coli* and purified from inclusion bodies in their misfolded GSSG oxidized states as previously described for the bovine oxytocin precursor and its derivative NP (*15*). Also as with the bovine oxytocin system, crude expression products had high fractional contents of covalently damaged protein, compromising ultimate yields of correctly folded protein **(**Results). CNBr cleavage and separation of the two components of the cleavage reaction were performed as previously described (*15*). Yields of precursor and NP constructs at this stage were ∼20 and 30 mg/L, respectively. In the case of the ^{VP}HNP-CP construct, which retained the Met in position 2 of NP, two products resulted from CNBr treatment. One product began with Ser-3 of NP, while the second began with Ala-1 and represented incomplete cleavage after Met-2, a known consequence of CNBr reaction with Met-Ser bonds (e.g., ref *16*). No difference in the properties of the two components was observed.

Folding of the expressed proteins involves reshuffling of multiple disulfides. Constructs not containing the hormone segment were folded at 1 mg/mL, pH 8 as previously described for ^{Oxy}BNP (*17*, *20*) using β-mercaptoethanol to facilitate disulfide rearrangement and exogenous peptide that binds to the hormone-binding site (Phe-TyrNH_2 or Phe-PheNH_2) to drive folding; the peptide concentration used (10 mM) represents the maximum compatible with solubility at pH 8. Folded protein was separated from unfolded protein by affinity chromatography (*20*). The purity and structures of the binding-competent proteins so isolated were respectively confirmed by native gel electrophoresis and mass spectrometry (MALDI).

For precursor folding, internal interactions between the covalently attached hormone and NP provide the thermodynamic driving force for folding and no peptide is added (*15*). Folding of the full-length precursor (HVP) in Tris-acetate buffer was attempted by stirring in air at pH 8 in the presence of β-mercaptoethanol or cysteamine, and by incubating at pH 7.4 with varying GSH/GSSG ratios (e.g., refs *15* and *18*). These conditions were accompanied by massive precipitation even at protein concentrations of 0.2 mg/mL, and no reproducible evidence of significant protein folding was obtained.

By contrast, significant folding was achieved of precursor from which CP was deleted (HVPΔCP). Best results were obtained with the β-mercaptoethanol procedure described above, omitting peptide and using a reduced protein concentration (0.2 mg/mL), folding yields diminishing with increased protein concentration. After 48 h, the protein was dialyzed against 0.2 M acetic acid and lyophilized prior to HPLC (vide infra). Folding was also achieved at low protein concentrations in a closed unstirred glutathione redox system at pH 7.4 in Tris-acetate buffer (*18*) with 3 mM each GSH and GSSG, these concentrations giving better results than the 20 mM GSH, 3 mM GSSG optimal for the oxytocin precursor (see Discussion). Protein folded in this way was directly used for HPLC to avoid complications noted from low pH dialysis in the presence of GSH prior to lyophilization. This method involved extensive HPLC time, but was less subject to random variation than the β-mercaptoethanol procedure.

Folding of the 87STOP and 90STOP precursors was optimally achieved using the same conditions as used for HVPΔCP, although higher protein concentrations could be used without precipitation during the folding reaction. This reflected a higher solubility of the misfolded form under folding conditions, and much of the misfolded form could be precipitated by reduction of the pH to 4.5 after completion of folding (Results).

Final purification of the folded forms of HVPΔCP and its 87STOP and 90STOP mutants was achieved by reverse phase HPLC using a semipreparative Vydac 218TP510 C_{18} column with a flow rate of 3 mL/min and a program beginning with a 10 min wash of 100% solvent A (0.1% TFA in water), followed by a gradient beginning with 75% A and 25% B (0.1% TFA in acetonitrile) and increasing to 60% A and 40% B over a 40 min period; the gradient was followed by a 5 min wash with 100% B. The initial 10 min wash was omitted for samples not containing GSH or GSSG. Each correctly folded precursor eluted as a sharp peak at ∼17 min after the start of the gradient. In each case, a second folded component, representing approximately one-third the intensity of the first, eluted ∼2 min later in a peak overlapping with one of the unfolded species. While the major folded component had the correct mass, this second peak was ∼40 mass units heavier when analyzed by mass spectrometry. Upon native gel electrophoresis (see also below), the heavier peak derived from the 87STOP precursor migrated ∼10% more slowly to the anode at pH 9.5 than the principal folded species. Its identity remains to be determined. To the extent analyzed, its biophysical properties are similar, but not necessarily identical, to those of the major component. All studies reported here were carried out with the major component.

Quantitation of Protein Folding Efficiencies. For constructs lacking hormone, folded protein was quantitated by its ability to bind to a peptide ligand-linked affinity column (vide supra). Precursor folding was routinely quantitated either by HPLC as described above or more approximately by CD, the latter as previously described for the bovine oxytocin

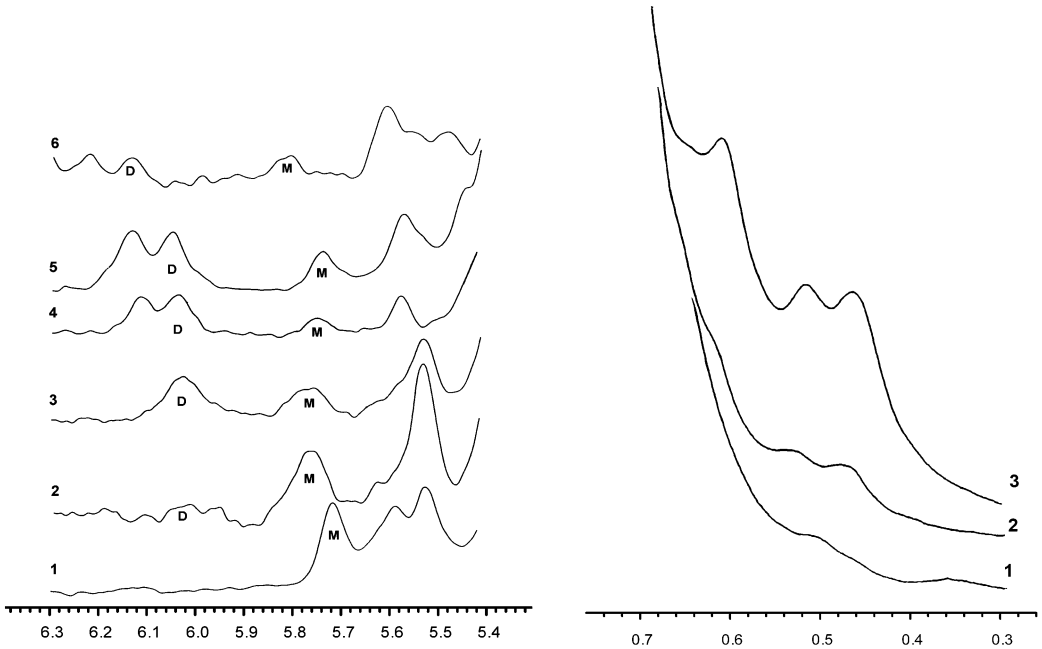

FIGURE 4: 600 MHz NMR spectra of ^{VP}HNP, ^{VP}HNP87STOP, and HVP87STOP. The abscissa is in ppm. Spectra were obtained in D_2O at 25 °C unless otherwise indicated. Left: In ascending order: (1) ^{VP}HNP87STOP, 0.2 mM, pH 6.4, 24 °C; (2) ^{VP}HNP, 0.05 mM, pH 6.2; (3) ^{VP}HNP, 0.3 mM, pH 6.2; (4) ^{VP}HNP, 0.05 mM + Phe-PheNH_2, pH 6.2; (5) ^{VP}HNP87STOP, 0.2 mM + Phe-PheNH_2, pH 6.4, 26 °C; (6) HVP87STOP (precursor), ~0.09 mM, pH 8.2. Signals labeled M and D are assigned as the monomer and dimer signals, respectively, from the Cys-28 α-proton. Dimer/monomer ratios increase with increasing concentration and binding. Right: In ascending order: (1) ^{VP}HNP87STOP, 0.2 mM, pH 6.4, 24 °C. (2) ^{VP}HNP, 0.05 mM, pH 6.2; (3) ^{VP}HNP, 0.3 mM, pH 6.2. Signals in the 0.4−0.52 ppm region are from dimer.

precursor (*15*), in this case using the 240/280 nm ellipticity ratio (as opposed to 240/290 nm) to estimate the fraction of folded protein in mixtures of folded and unfolded protein. Assumed 240 nm molar ellipticities were +30 000 and −33 000 for folded and misfolded states respectively and assumed 280 nm molar ellipticities were −12 000 for both folded and unfolded states.

Folding Kinetics. Folding of NPs from the reduced state was monitored by CD in Tris-acetate buffer at pH 7.4 and 25 °C in the presence of ligand dipeptides and 2 mM each GSH and GSSG using nitrated protein as previously described (*18*). Rates of precursor folding from the GSSG-oxidized CNBr-cleaved expression product were determined by HPLC in Tris-acetate buffer at pH 7.4 and 37 °C in the presence of 3 mM each GSH and GSSG.

Dimerization. Dimerization constants were principally determined by NMR in D_2O at 600 MHz as previously described (*9, 19*); pH values are uncorrected meter readings. This method utilizes the relative intensities of the α-proton signal of NP Cys-28 in monomeric and dimeric states to calculate the fractional content of monomer and dimer. In the case of ^{VP}HNP (Figure 4), the Cys-28 proton gives rise to single signals located at 5.75 and 6.03 ppm in the unliganded monomer and dimer, respectively, which can be compared with values of 6.2 and 6.4 ppm, respectively, in the bovine NPs (*9, 19*); as with the bovine NPs, these shifts are largely unperturbed by ligand binding (*20*). Chemical shifts in other constructs (e.g., Figure 4) were similar but nonidentical. Note that a signal at ~6.12 ppm in the liganded state is currently assigned to a proton other than that from Cys-28 because this assignment is the most consistent with the fraction of protein in the liganded state. However, conclusions are not qualitatively altered by the alternative assignment because the same assumptions are made for all proteins.[2]

NMR signals from NP-CP were not as distinct as those in other constructs. Dimerization constants for NP-CP were accordingly also approximated by sedimentation equilibrium in the analytical ultracentrifuge as previously described (*20*) and measuring the effect of different loading concentrations on the average molecular weight in the cell.

Electrophoresis. SDS and native gel electrophoresis were performed as previously described (e.g., ref *15*). The native gel system, in which proteins enter the gel at pH 8.3 and run to the anode at pH 9.5, could be used to monitor the purity/folding of most preparations (e.g., ref *15*), but not of HVPΔCP, which is too basic to enter the gel under these conditions.

Other Methods. Essentially all other methodology has been described earlier. A Jasco J-710 spectrometer was used for CD studies. Peptide-binding studies were performed by fluorescence (*20*). Guanidine denaturation studies were performed at 25 °C by the addition of solid guanidine hydrochloride to the folded protein and analyzed using a two-state denaturation model, both as previously described (*9*). Details of other studies are given in Results and/or in table legends.

[2] The alternative assignment would in part necessitate a greater than 10-fold difference in the relative binding affinities of monomeric and dimeric chains and, accordingly, a higher dimerization constant of the liganded state than assumed here. The principal effect of this on the conclusions here would be to further reduce the calculated binding affinity of the monomeric state and hence its calculated stability.

Table 1: Properties of Human and Bovine Vasopressin-related Neurophysins

	^{VP}BNP	^{VP}HNP	^{VP}HNP87STOP	^{VP}HNP-CP
$\Delta G_{\text{guanidine denaturation}}$ (kcal/mol)[a]	2.3 ± 0.2	2.5 ± 0.2	2.2 ± 0.1	2.1 ± 0.2
$K_{\text{Phe−Phe−amide}}$ (mM^{-1})[b]	8.2 (±0.3)	2.2 (±0.4)	4.9 (±0.1)	
folding rate constant (min^{-1})	2.5×10^{-3}	5.1 (±0) $\times 10^{-3}$	2.0 (±0.7) $\times 10^{-3}$	
dimerization constant pH 6.2 (mM^{-1})[c]	5.4 (±1.8)	4.2 (±0.6)	0.3−1 (0.8)	16 (±7) 14 (±3)[d]
dimerization constant pH 7.5 (mM^{-1})[e]	5.1	2.3 (±0.3)		13 (±3)

[a] Data for the human proteins were obtained at pH 6.2 and 25 °C at protein concentrations of ~0.06 mM for ^{VP}HNP, 0.04 mM for ^{VP}HNP87STOP, and 0.03 mM for ^{VP}HNP-CP. Data for ^{VP}BNP are from ref 9 and were obtained at a concentration of 0.1 mM in the pH range 6.2−8. [b] Determined by fluorescence at pH 6.2 and protein concentrations of 0.05 mM. The value for ^{VP}BNP was redetermined for this study. [c] Unless otherwise indicated, dimerization constants reported are those determined by NMR for the unliganded proteins at pH 6.2 (uncorrected pH meter reading) in D_2O. The dimerization constant of ^{VP}BNP so determined is that previously reported by this method and is the same as that calculated from ultracentrifuge data (*19*). The dimerization constant of the 87STOP mutant was estimated from NMR data as described in the text. [d] Determined by analytical ultracentrifugation at pH 6.2 in 0.1 M ammonium acetate, 2 mM Mes buffer. [e] The bovine protein results represent published analytical ultracentrifugation studies at pH 7.5 (*21*); no statistics were reported. Other pH 7.5 values represent NMR data.

RESULTS

Properties of Human Vasopressin-Related NP (^{VP}HNP). The properties of ^{VP}HNP merit comparison with those of ^{VP}BNP, which, because of its solved crystal structures, has been the principal paradigm of neurophysin structure−function relationships (e.g., ref *10*). A single round of β-mercaptoethanol folding of the CNBr-cleaved ^{VP}HNP expression product yielded ~20% folded ^{VP}HNP, the low folding efficiency shown in large part to reflect the presence of covalently damaged protein (Methods) and also in this case the inefficient folding of undamaged protein. The latter situation differs from the more complete folding of ^{VP}BNP under the same conditions (*17*), the difference probably reflecting the lower affinity of ^{VP}HNP than of ^{VP}BNP for Phe-PheNH_2 (Table 1), the ligand used to drive folding. Consistent with the different peptide affinities, preliminary comparison of the CD spectra of purified folded ^{VP}HNP and ^{VP}BNP suggests conformational differences between the two proteins, which remain to be defined (data not shown).

Table 1 compares properties of ^{VP}HNP with those of ^{VP}BNP reported earlier and/or redetermined for this study (see table legend). With the exception of the lower peptide affinity of ^{VP}HNP and an effect of pH on ^{VP}HNP dimerization, differences between the two proteins are unremarkable. Figure 4 shows representative NMR data, from which the dimerization constants of ^{VP}HNP in Table 1 were calculated, illustrating the effects of concentration on the dimerization-sensitive resonances (Methods) of ^{VP}HNP and other constructs. The small decrease in dimerization constant between pH 6.2 and 7.5 (Table 1) is assigned to titration of His-90, the environment of which is shown by NMR to be sensitive to the degree of dimerization of the protein (Figure 5) and which can similarly be seen to titrate in this pH region (data not shown). This assignment is supported by the pH independence in this region of the dimerization constant of ^{VP}BNP (Table 1), which has no histidine (Figure 1). The human protein also exhibited the expected increase in dimerization constant (*21*, *22*) in the liganded state. NMR studies (Figure 4) demonstrated that a 0.05 mM solution of ^{VP}HNP at pH 6.2 (~25% dimer by weight in the unliganded state) was converted to 68% dimer by weight when ~75% saturated with Phe-PheNH_2, representing an increase in the average dimerization constant from 4×10^3 M^{-1} (Table 1) to 6.8×10^4 M^{-1}.

Effect of Copeptin Attachment on the Properties of ^{VP}HNP: *Properties of ^{VP}HNP-CP*. Yields of folded ^{VP}HNP-CP obtained from the crude CNBr product were similar to that of ^{VP}HNP alone. Solubility problems with the peptide complexes of ^{VP}HNP-CP, and with the nitrated form of ^{VP}HNP-CP in general, prevented direct determination of peptide binding constants. However, because peptide affinity is a limiting factor in the folding of ^{VP}HNP under our conditions (vide supra), the generally similar folding efficiencies of ^{VP}HNP-CP and ^{VP}HNP suggest that copeptin does not significantly affect binding affinity.

Protein	Dimerization constant (M^{-1})
Bovine ^{VP}NP	5×10^3
Des 1-6 Bovine ^{VP}NP	24×10^3
Des 1-6, 87-95 Bovine ^{VP}NP	6.5×10^3
Human ^{VP}NP	4.2×10^3
Human ^{VP}NP87STOP	~0.8×10^3

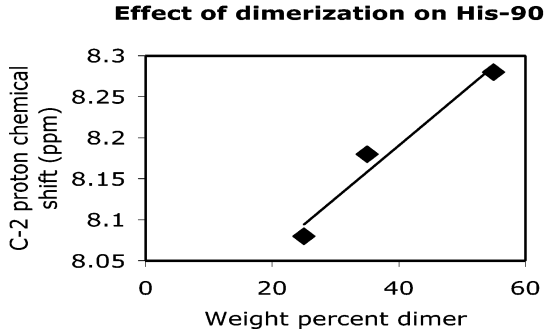

FIGURE 5: Role of the C-terminus of ^{VP}HNP and of analogues of ^{VP}BNP in dimerization at pH 6.2. Data for the bovine proteins are from ref 9. The graph shows the effect of dimerization at pH 6.2 on the chemical shift of the C-2 proton of His-90 of ^{VP}HNP.

Several other properties of ^{VP}HNP-CP are shown in Table 1. The most notable is a 3−4-fold increase in dimerization constant and a possible reduction in the pH dependence of dimerization compared to ^{VP}HNP alone, suggesting either direct or indirect interaction between NP and CP components. The measured lower stability of ^{VP}HNP-CP than of ^{VP}HNP in Table 1 is relevant in this context. At the concentrations at which the stabilities of these components were measured (see table legend) the dimer content of ^{VP}HNP-CP is higher than that of ^{VP}HNP. The fact that the increased dimerization is accompanied by a trivial stability decrease, rather than an expected (see Discussion) stability increase, suggests the possibility of a small destabilization of NP structure by CP.

Effect of the 87STOP Mutation on the Properties of ^{VP}HNP. The folding efficiency of ^{VP}HNP87STOP (~25% relative to starting material) was trivially higher than that of ^{VP}HNP. Comparison of the properties of ^{VP}HNP87STOP with those of ^{VP}HNP demonstrated that loss of the C-terminal seven residues from ^{VP}HNP led to an increase in binding constant for Phe-PheNH$_2$ (possibly accounting for the increase in folding efficiency), a reduction in folding rate and a markedly reduced dimerization constant (Table 1). The reduction in folding rate is of doubtful significance because it does not lead to a lower folding efficiency and is not paralleled by a slower folding rate of the 87STOP precursor when the corresponding precursors are compared (vide infra). The reduction in dimerization constant is illustrated in Figure 4, which shows that no Cys-28 dimer signal is present in the mutant at a concentration of 0.2 mM, while one is weakly visible in ^{VP}HNP at a concentration of 0.05 mM. Upfield spectra (Figure 4) similarly show that less dimer signal intensity is present in the mutant despite its 4-fold higher concentration; signals at 0.46 and ~0.53 ppm are present only in the dimeric state. The results can be shown to indicate a dimerization constant in the range $0.3-1 \times 10^3$ M^{-1}, a value 7−24% that of ^{VP}HNP under the same conditions, and point to a significant modulating effect of residues 87−93 on dimerization. Nonetheless, the increase in dimerization associated with ligand-binding is preserved in the mutant. At a protein concentration of 0.2 mM, 70% saturation with Phe-PheNH$_2$ increased the measured average dimerization constant to 1.2×10^4 M^{-1} (Figure 4), the increased value again only 18% that of ^{VP}HNP at a similar state of ligation (vide supra). The results are consistent with an ~80% reduction in dimerization constant at pH 6 by the 87STOP mutation in both unliganded and liganded states. The measured difference in stability to guanidine denaturation of ^{VP}HNP and its 87STOP mutant (Table 1) is largely accounted for by this effect (e.g., Appendix).

Folding Studies of the Full-Length Human Vasopressin Precursor (HVP). No reproducible folding of HVP was detected under our conditions (Methods). This was true for constructs containing either Leu or Ala in NP position 2, supporting the view that this position does not play a significant role in folding. The precipitate formed during attempts to fold HVP (Methods) required both guanidine·HCl and reduction for solubilization, suggesting the presence of extensive intermolecular cross-linking. Attempts to solubilize insoluble folding intermediates by the addition of low concentrations of guanidine·HCl during folding, or to fold from the completely reduced state, were unsuccessful. Addition of 1 M proline, which binds to folding intermediates (*23*), completely prevented precipitation, but did not increase folding under our conditions.

Folding Properties of HVPΔCP and Its 87STOP Mutant. By contrast with HVP, both HVPΔCP and its 87STOP mutant folded under our conditions, although yields of folded protein were approximately a third of those of the folded oxytocin precursor. The folding of HVPΔCP indicates that CP attachment is responsible for the failure of HVP to fold, a result that contrasts with the failure of CP to affect the folding of the corresponding NPs. Yields of folded HVPΔCP and its 87STOP mutant were lower than found for the corresponding NPs, a situation similarly observed with the oxytocin precursor that reflects folding pathway problems introduced by the hormone's disulfide (*15*, *18*). Thus, the different effects of CP on precursor and NP folding may reflect pathway differences.

Table 2: Folding Properties of HVPΔCP and HVP87STOP in Glutathione Redox Buffer

	HVPΔ*C*P	HVP87STOP
decrease in folding efficiency upon increasing the temperature from 25 to 37 °C *(%)*[a]	0.4 ± 0.4	25 ± 11
decrease in folded protein upon reincubation in folding buffer at 37 °C[b]		
pH 7.1 (%)	33 ± 4	31 ± 7
pH 7.4 (%)	46 ± 7	57 ± 3
first-order folding rate constant at pH 7.4 and 37 °C (min^{-1})[c]	1.2 (±0.4) × 10^{-2}	1.6(±0.7) × 10^{-2}

[a] Protein (0.5 mg/mL) from a single CNBr-cleaved expression product was folded in the presence of 3 mM each GSH and GSSG in Tris-acetate buffer, pH 7.4 at 25 °C (Methods) and in the identical buffer at 37 °C (pH 7.1 at 37 °C). Folding was quantitated by HPLC. [b] Purified folded protein at concentrations of ~2×10^{-6} M was reincubated for 24 and 48 h at 37 °C in the above glutathione system at the pH values (at 37 °C) indicated. The quantity of folded protein relative to a similarly incubated control lacking glutathione was determined by HPLC and, for the 87STOP mutant, also was monitored by native gel electrophoresis (Methods). Results at pH 7.1 are averages (± SE) of multiple studies. Results at pH 7.4 are from a single study, with an estimated uncertainty reflecting different methods of HPLC peak integration. [c] The rate of folding of CNBr-cleaved expression products in the glutathione system was monitored by HPLC. Conditions were 37 °C, pH 7.4, 0.5−1 mg/mL HVPΔCP and 0.2 mg/mL 87STOP mutant. The higher concentration of HVPΔCP used was necessitated by a particularly high concentration of damaged (folding-incompetent) protein in this expression product.

At best, folding yields provided only ambiguous evidence of differences between HVPΔ*C*P and the 87STOP mutant and hence of a potential role in folding of the seven C-terminal NP residues. Under identical room temperature folding conditions, approximate yields of folded 87STOP and WT proteins from their CNBr-cleaved expression products were 8 and 13%, respectively, using the β-mercaptoethanol procedure, but yields were equivalent or slightly higher for the mutant using the glutathione procedure. To further test the relative folding efficiencies of the two precursors and to examine temperature effects, we compared the effects of temperature on the folding efficiencies of individual lots of expression product (Table 2), in this case folding each lot with the GSH/GSSG buffer system at pH 7.4 and 25 °C and in the same buffer at 37 °C (pH 7.1 at 37 °C). This approach in principle both removed the experimental variability of the β-mercaptoethanol procedure (Methods) and canceled out effects of differences among preparations in folding-incompetent protein. As shown in Table 2, moderate but variable differences between the proteins were seen, folding of the 87STOP mutant on average appearing to decline more with temperature than that of HVPΔ*C*P.

More reproducible results were obtained from examination of the folding/unfolding equilibria of the two precursors at 37 °C, at low protein concentration, in the glutathione buffer system (Table 2). Specifically, the change in concentration of folded protein was measured when the purified folded

precursors were reincubated in the redox buffer at pH 7.1 and 7.4 (the pH values at 37 °C) for 24 and 48 h. No significant differences between the 24 and 48 h results were found, indicating that an equilibrium was attained. Approximately 30% of both proteins unfolded at 37 °C and pH 7.1, the conditions used for the above studies of the temperature-dependence of folding (Discussion). The percentage of unfolded protein increased to ~50% at pH 7.4 and 37 °C, with a possible indication that the mutant might be slightly less stable than HVPΔCP at the higher pH. Folding rates of the two proteins in the glutathione system were similar (Table 2). The rate and equilibria studies therefore indicated more of a similarity between the two proteins than a difference and, most significantly, demonstrated a folding equilibrium for both proteins that is not strongly in favor of the folded form under the conditions used. Potential sources of discrepancies between the variable relative folding efficiencies of the two proteins and their similar folding equilibria are given in Discussion.

Other Thermodynamic Studies of HVPΔCP and Its 87STOP Mutant. The similarity and relative instability of the two precursors were also suggested by other properties. A central contributor to precursor stability is the strength of internal interaction between hormone and NP (*15*). The near-ultraviolet CD spectrum of purified folded HVPΔCP is shown in Figure 6, together with that of its derivative NP; spectra of the corresponding mutant proteins are analogous (figure legend). Differences between the spectrum of the precursor and that of its derivative NP are similar to those associated with the intermolecular binding of VP to ^{VP}BNP (*24*), as previously observed for the relationship between the CD spectrum of the bovine oxytocin precursor and that of the intermolecular complex between ^{Oxy}BNP and oxytocin (*15*, *25*). As also found for the bovine oxytocin precursor (*15*), the internal interactions between hormone and NP in HVPΔCP and its 87STOP mutant dissociate at elevated pH, due principally to competition between deprotonation of the hormone α-amino group in the unliganded state and binding of the protonated amino to the NP segment. Figure 6 also shows the CD effects of titrating HVPΔCP and its 87STOP mutant between pH 7 and 11. Because ionization of Tyr-49 of ^{VP}HNP can be shown to be unaccompanied by significant CD changes in the 240−340 nm region, the decrease between pH 7 and 11 in 240 nm ellipticity and changes in the 280/290 nm ellipticity ratio solely reflect loss of the normal hormone interaction with the NP binding site (*15*, *25*). The titration results therefore indicate a midpoint of hormone−NP dissociation within experimental error of 9.5 for both precursors. As with the oxytocin precursor (*15*), the difference between this pH and the pK_a of the unbound hormone (independently determined as 6.3 at 25 °C, the same as that of oxytocin) is a measure of the intraprecursor binding constant to NP of hormone in which the α-amino group is completely protonated in the unbound state, where

$$\Delta G_{\text{Binding}} = -2.3RT(\text{pH} - \text{p}K_a) \qquad (1)$$

The internal binding constant for protonated VP is calculated as 1585 at 25 °C, which compares with a titration-derived value of 5000 (±3000) in the oxytocin precursor (*15*).

HVPΔCP and its 87STOP mutant were also compared by measuring their susceptibility to denaturation by guanidine·HCl (Table 3). Analysis of the pH 6.2 data using a two-state denaturation model (*26*) gave values for both proteins approximately 1.5 kcal/mol lower than that obtained (Table 3) for the oxytocin precursor at pH 6. As with the oxytocin precursor, the 2 kcal/mol decrease in precursor stability between pH 6 and pH 8 reflects the increased deprotonation of the hormone amino group in the unliganded state at the

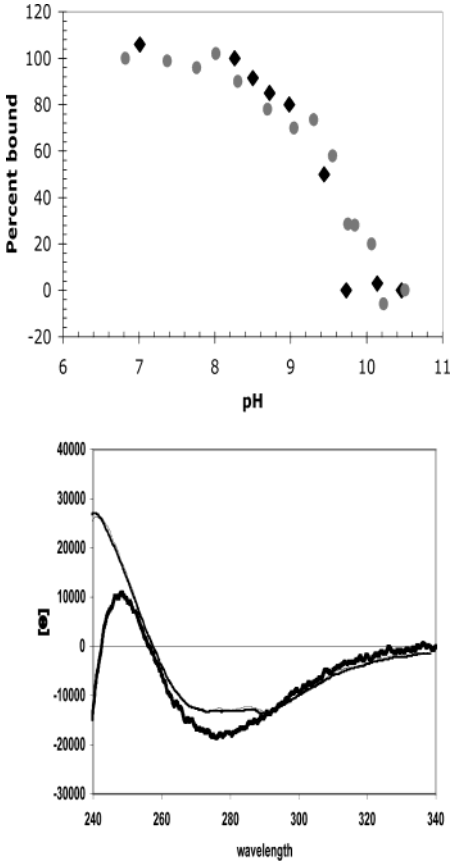

FIGURE 6: Lower: Comparison of the near-ultraviolet CD spectra of ^{VP}HNP, HVPΔCP, and HVP87STOP at neutral pH. Ordinate is molar ellipticity; abscissa is in nanometers. Heavy line, ^{VP}HNP. Light lines (largely superimposed), HVPΔCP and HVP87STOP. The spectrum of ^{VP}HNP87STOP (not shown) is the same in this region as that of ^{VP}HNP. Upper: Effect of pH on the internal binding of hormone to NP in HVPΔCP (black diamonds) and HVP87STOP (grey ovals) at 25 °C. Protein concentration = 0.05 mM. Data plotted are averages of the pH-induced changes at 240 nm and in the 280/290 nm ratio.

Table 3: Comparison of the Stabilities to Guanidine Denaturation of HVPΔCP and HVP87STOP and Their Derivative NPs with Those of the Bovine Oxytocin Precursor and Its Derivative NP[a]

	Δ*G*° (kcal/mol)		*m* (kcal mol^{-1} M^{-1})	
	pH 6.2	pH 8	pH 6	pH 8
HVPΔCP	5.3 ± 0.7	3.3 ± 0.2	1.4 ± 0.2	1.0 ± 0.04
^{VP}HNP	2.5 ± 0.2	*2.46*[b]	0.63 ± 0.14	*0.63*[b]
HVP87STOP	5.4 ± 0.1	N. D.	1.49 ± 0.06	N. D.
^{VP}HNPSTOP	2.2 ± 0.1	N. D.	0.61 ± 0.04	N. D.
^{Oxy}BNP precursor[c]	6.8 ± 0.4	4.9 ± 0.1	1.6 ± 0.1	1.5 ± 0
^{Oxy}BNP[c]	3.1 ± 0.1	3.0 ± 0.35	1.1 ± 0.1	1.1 ± 0.1

[a] Conditions: measured in 0.1 M ammonium acetate at 25 °C with protein concentrations of 0.050 ± 0.01 mM. [b] Value of Δ*G*° (kcal/mol) is that calculated in Table 4 at pH 7.4. Value of "m" is assumed. [c] Data are from ref *15*. Note that the pH in these studies is 6.0, not 6.2, but that this difference accounts for only 0.11 Kcal of the difference between the VP and oxytocin precursors.

higher pH (*15*); note that changes in dimerization due to deprotonation of His-90 are too small to significantly affect stability at these concentrations, titration of His-90 does not significantly affect binding affinity (data not shown), and no other group titrates in this pH region. However, while the hormone remains essentially completely liganded at pH 8 (Figure 6), the "m" value (*26*) of HVPΔCP at pH 8 is lowered to a value intermediate between that at pH 6 and that of its component NP. This indicates that, at pH 8, guanidine induces dissociation of about half of the internal hormone−NP interactions prior to unfolding of the precursor as a whole, i.e., the unfolding pathway involves at least three states. This is not seen to the same extent with the oxytocin precursor at this pH, possibly reflecting the higher internal binding constant of the oxytocin precursor. Nonetheless, as with the oxytocin precursor (*15*), measured stabilities at pH 6.2 are ∼1 kcal/mol less than that estimated (Discussion) from the sum of the stabilities of the NP components of the precursors and the free energy of internal hormone−NP interaction at this pH (∼6.6 kcal/mol for HVPΔCP and 6.3 kcal/mol for 87STOP). A potential source of the discrepancy is the inapplicability of a two-state model to guanidine-induced precursor denaturation even at pH 6. That is, the unfolding profile is viewed as containing contributions both from the two-state unfolding (with hormone dissociation) of the internally liganded precursor and from the three-state mechanism detected at pH 8, the relative contribution of the three-state mechanism increasing with pH, but still significant at pH 6.

Role of the Carboxyl Terminus in Precursor Solubility Properties. The principal difference seen between HVPΔ*C*P and its 87STOP mutant was the solubility of their misfolded forms, either as obtained from the folding of the crude expression products or the refolding of the purified reduced proteins. The misfolded form of HVPΔCP precipitates out with high efficiency during folding reactions, CD spectra of the pH 7.4 or pH 8 supernatants indicating low concentrations of a product containing a high percentage of folded protein (Figure 7). Like the insoluble HVP folding products, the precipitate can be resolubilized only by reduction in the presence of guanidine, this property and the inverse concentration-dependence of folding efficiency indicating the presence of intermolecular disulfide cross-linking of the misfolded states. By contrast, the misfolded form of the 87STOP precursor is much more soluble under folding conditions, so that spectra obtained of folding reactions of the mutant precursor are dominated by contributions of misfolded species, the latter removable by precipitation at pH 4.5 (Figure 7). Significantly, the 90STOP mutant of the precursor exhibits the same solubility properties as the 87STOP mutant (Figure 7**)** indicating that HRRA, the last four residues of HVPΔCP (Figure 1), are responsible for the insolubility.

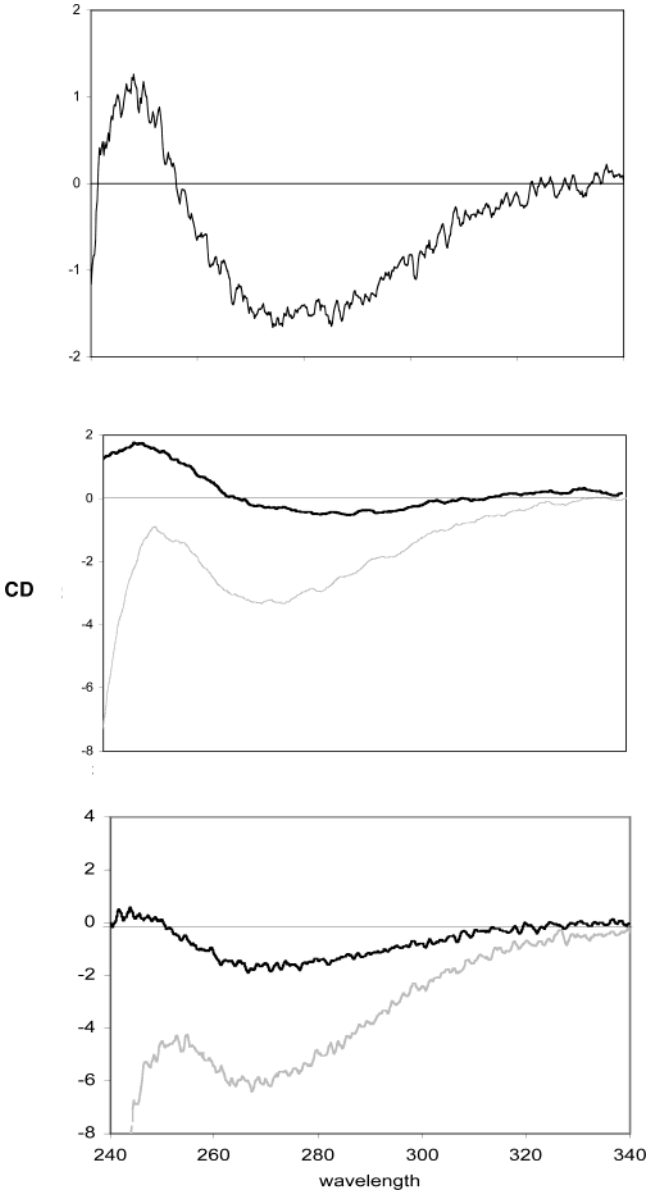

FIGURE 7: CD spectra in the near UV of the solution supernatants of HVPΔCP, and its 87STOP and 90STOP mutants, obtained after folding in the presence of β-mercaptoethanol at pH 8. Top: HVPΔCP, pH 8, 2-cm light path. Sample was folded at 0.2 mg/mL. Spectrum is not significantly changed after precipitation at pH 4.5 (not shown). Center: 90 STOP mutant, 0.5-cm light path. Grey, pH 8. Black, after precipitation at pH 4.5. Sample was folded at 0. 5 mg/mL. Bottom: 87STOP mutant, 0.5-cm light path. Grey, pH 8. Black, after precipitation at pH 4.5. Sample was folded at 1 mg/mL. Spectra obtained at pH 8 indicate ∼100% solubility of both mutant proteins in the pH 8 supernatant, while only 33% of HVPΔCP is found in the pH 8 supernatant despite the markedly lower concentration used for folding. CD units are millidegrees.

DISCUSSION

The central question is the identity of factors that selectively decrease the folding efficiency of the human 87STOP precursor and thereby contribute to its pathogenicity. The above results establish that the seven NP residues deleted by the 87STOP mutation alter dimerization, the solubility of misfolded precursor states, and, as discussed further below, peptide affinity. However, while these effects are of mechanistic interest and may play secondary roles in pathogenicity (vide infra), they do not appear to be the primary cause of mutant misfolding**.** With respect to dimerization, a decrease in dimerization constant associated with termination of the protein at residue 86 was also seen earlier in both unliganded bovine neurophysins (*9*), but the potential significance of the effect was unclear; the decrease was relatively small in the case of ^{Oxy}BNP and was based on studies of an amino-truncated derivative in the case of ^{VP}BNP (ref *9* and Figure 5). The dimerization decrease is unambiguous in the case of ^{VP}HNP because it is particularly large at pH 6 and paralleled

Table 4: Calculation of Thermodynamically Allowed Folding Efficiencies

	HVPΔCP	HVP87STOP
(a) $K_{\text{binding protonated hormone, 25 °C, 0.05 mM}}$[a]	1585	−1585
(b)$K_{\text{binding, monomer, pH 7.4, 37 °C}}$[b]	10.6	15.5
(c) $K_{\text{intrinsic binding, dimer subunit, pH 7.4, 37 °C}}$[c]	108	169
(d) $\Delta G_{\text{binding, pH 7.4, 37 °C, monomer}}$[d] (kcal/mol)	−1.49	−1.73
(e) $\Delta G_{\text{binding, pH 7.4, 37 °C, 0.1 M (dimer)}}$[e] (kcal/mol)	−2.95 (×2)	−3.2 (×2)
(f) $-\Delta G_{\text{NP denaturation, pH 7.4, 25 °C, 0.05 mM}}$[f] (kcal/mol)	−2.46	−2.20
(g)$-\Delta G_{\text{NP denaturation, pH 7.4, 37 °C, monomer}}$[g] (kcal/mol)	−2.20	−2.12
(h) $-\Delta G_{\text{NP denaturation, pH 7.4, 37 °C, 0.1M (dimer)}}$[h] (kcal/mol)	−6.09	−5.37
(i) $-\Delta G_{\text{precursor denaturation, pH 7.4, 37 °C, monomer}}$ (kcal/mol)	−3.69	−3.85
(j) $-\Delta G_{\text{precursor denaturation, pH 7.4, 37 °C, 0.1 M dimer}}$ (kcal/mol)	−11.99	−11.77
(k) precursor folding efficiency$_{\text{pH 7.4, 37 °C, monomer}}$ (%)	75	79
(l) precursor folding efficiency$_{\text{pH 7.4, 37 °C, 0.1 M (dimer)}}$ (%)	99.8	99.8

[a] Intramolecular binding constant of hormone in which the α-amino group is completely protonated in the unbound state (e.g., ref *15*), determined at 25 °C, 0.05 mM precursor concentration from the data in Figure 6 as described in the text. [b,c] Derived from the pH dissociation curve in Figure 6 as described in the appendix. [d] Represents the free energy of binding to monomer at infinite dilution such that no dimer is formed, and is the free energy equivalent of (b). [e] Represents the free energy of binding to the two dimer sites under conditions (0.1 M chain concentration) in which the protein is essentially all dimer in both unliganded and liganded states and is calculated per site as the free energy equivalent of (c). Contributions of the small changes in dimer content that do accompany binding can be shown to negligible at 0.1 M. [f] Values obtained from guanidine denaturation studies at pH 6 and 25 °C (Table 1) corrected for the difference in dimerization between pH 6 and 7.4 for 0.05 mM HVPΔCP, by subtracting the pH 6 contribution and adding the pH 7.5 contribution using eq 3 in the appendix. No correction for temperature is made. [g] Calculated from (f) by subtracting the free energy of dimerization at 0.05 mM using eq 3. [h] Calculated from (g) by adding the free energy of dimerization at 0.1 M using eq 3. [i] Sum of (d) and (g). [j] Sum of (e) and (h). [k,l] Folding efficiencies are calculated by subtracting 3 kcal/mol from the free energies in (i and j), the difference representing the free energy advantage of the correctly folded state relative to misfolded states (Discussion).

by the sensitivity of His-90 to dimerization. However, its potential contributions to mutant stability are shown below to be offset by the attendant increase in binding associated with the mutation.

With respect to solubility, the deleted "insolubilizing" sequence XRRX is conserved in most mammalian VP precursors (e.g., ref *27*), but its absence cannot in itself be pathogenic since it is absent, for example, in the WT rat VP precursor (Figure 1) as well as in WT oxytocin precursors (*27*), and the solubility properties of misfolded WT bovine oxytocin precursor states (Eubanks, S., and Breslow, E., unpublished experiments) mirror those of HVP 87STOP. Nonetheless, the greater solubility of misfolded forms of the 87STOP precursor than of HVPΔCP might be an important contributor to the contrast between their variably different in vitro folding efficiencies and their similar thermodynamic properties (Results). The fact that precursor folding efficiency decreases with increasing concentration (Methods) is consistent with kinetic competition between folding and aggregate formation. During HVPΔCP folding, aggregated misfolded species are isolated by their insolubility from the remaining protein, which is not the case for the 87STOP mutant. At the same initial protein concentration, to the extent that aggregated soluble species are reactive, some fraction of the 87STOP mutant accordingly folds at an effectively higher concentration than HVPΔCP, the difference between the two affected by the different factors (e.g., stirring rate, temperature) that influence solubility and rates of precipitation.

Our data reveal no material stability differences between HVPΔCP and the 87STOP precursor, as monitored either by guanidine denaturation, pH effects, or folding/unfolding equilibria in a glutathione redox buffer. However, both precursors were found to undergo significant redox buffer mediated unfolding at physiological pH and temperature under our experimental conditions. To probe the origin of the instability and its relationship to in vivo folding, we independently calculated the thermodynamically allowed folding efficiencies of the monomeric and dimeric forms of HVPΔCP and its 87STOP mutant, from the reduced state, at physiological pH and temperature. These calculations solely used the *other* thermodynamic data acquired here, together with properties of the NP-precursor system demonstrated earlier. Calculation details are given in the appendix and Table 4 legend, with the principal features of the calculations explained as follows.

The calculations predict folding efficiencies by utilizing a relationship that can be established in this system between the stability to guanidine denaturation and the efficiency of folding from the reduced state (vide infra). Because the measured stabilities of the precursors to guanidine denaturation appear to be underestimates, stabilities are calculated indirectly, using the assumption (*15*) that the stability of the precursor to guanidine denaturation is the same as the stability to guanidine denaturation of its NP component in the unliganded state plus the free energy of internal NP−hormone interaction, i.e.,

$$-\Delta G_{\text{precursor denaturation}} = -\Delta G_{\text{NP denaturation}} + \Delta G_{\text{binding}} \quad (2)$$

In the case of the oxytocin precursor, the discrepancy between observed precursor stabilities and those predicted by eq 2 raised the question as to whether the covalent linkage between hormone and NP in the precursor altered the stability of the NP component in the absence of noncovalent hormone−NP interactions (*15*), thereby invalidating eq 2 assumptions. This is not the case. In unpublished studies, we demonstrated that the stability of the oxytocin precursor to guanidine denaturation is identical to that of its NP component at pH values at which noncovalent hormone−NP interactions are absent. Accordingly, the discrepancy more likely reflects the inapplicability of a two-state model to guanidine-induced precursor denaturation, as discussed above. However, to the extent that stability values derived directly from precursor guanidine denaturation studies might in fact be more accurate, our calculations, which yield higher stabilities, overestimate folding efficiency.

The relationship we use between guanidine denaturation stability and the thermodynamics of folding from the reduced

state derives from earlier studies (*18*) demonstrating that, in the redox system used here, unliganded NP folds to a disulfide-mispaired state and a native state. For ^{VP}BNP, the misfolded state is thermodynamically favored relative to the correctly folded state by ~1 kcal/mol (*18*), while for ^{Oxy}BNP, the two forms have equivalent energies (*15*). The difference in relative stability of the two folded unliganded states is approximately the same as the difference between the two in their stabilities to guanidine denaturation, 2.3 ± 0.2 kcal/mol for ^{VP}BNP and 3.0 ± 0.1 kcal/mol for ^{Oxy}BNP under concentration conditions representing equivalent degrees of dimerization (*9*). Thus, we assume that ~3 kcal/mol stability to guanidine denaturation represents the stability required to obtain, on folding, an equal population of correctly folded and misfolded states. Stabilizing energy in excess of this is required to drive the folding reaction to completion.

Our calculations also make use of the demonstrations that bovine precursor dimerization properties closely mirror the dimerization properties of their component neurophysins in the liganded state (*11*, *28*), that negligible cooperativity between dimer subunits occurs on binding (*22*), and that the dimerization constants of the liganded states are ~100-fold greater than those of the unliganded states (e.g., 28), reflecting a 10-fold higher binding constant of a dimer subunit than of a monomer. These assumptions, together with the measured NP dimerization constants in the unliganded state, allow the individual intramolecular hormone−NP binding constants for the monomeric and dimeric states of the precursor to be obtained from the pH titration data.

The values in Table 4 represent estimates, obtained with the above assumptions, of the predicted stabilities to guanidine denaturation and the folding efficiencies at pH 7.4 and 37 °C of HVPΔCP and its 87STOP mutant in their purely monomeric states (infinite dilution) and in their essentially all dimer states at 0.1 M chain concentration; 0.1 M is the estimated hormone concentration within neurosecretory granules (*29*) and therefore the probable upper limit to precursor concentration at any point in the cell. These values allow preliminary insights into the range of stabilities experienced by the two proteins as they move from their initial site of folding in the ER to the higher concentrations at the cis-Golgi (*30*) and finally to neurosecretory granules**.** Concentration contributes to precursor stability (see also Appendix) because of its effects in eq 2 on the stability of unliganded NP (the stabilizing consequences of dimer formation) and on hormone−NP binding (stronger binding by dimers).

The predicted stabilities and folding efficiencies in Table 4 are probably maximum estimates because neither the dimerization constants nor the stabilities of unliganded NP to guanidine denaturation used are corrected from their 25 °C values (Appendix). Nonetheless, they represent evidence that, with respect to thermodynamics alone, folding efficiency will depend strongly on protein concentration, with 20−25% of the precursors unfolded at infinitely dilute (monomer) concentrations and ~0.2% predicted to be unfolded at 0.1 M concentration. The calculations are in significant agreement with the results of the "unfolding" studies in Table 2, which were carried out at concentrations at which dimer contributions are relatively small, in their prediction of inefficient folding by both precursors at low concentration; they can also be shown to predict the decrease in folding between pH 7.1 and pH 7.4 shown by the "unfolding" studies. The relatively small differences between calculated and observed results, moreover, are potentially attributable to the above approximations in the thermodynamic analysis. Because the GSH/GSSG ratio used for unfolding is the optimum ratio we found for folding (Methods) and represents redox potentials similar to those in the ER (e.g., ref *31*), the results also point to the instability of these proteins under conditions approaching those in the ER. Finally, it is noteworthy that the thermodynamic analysis explains the similar stabilities of both precursors, despite the higher dimerization constant of HVPΔCP, by demonstrating compensation by a higher NP−hormone binding constant in the 87STOP precursor (Table 4 and Appendix), a property apparently paralleling the effect of the 87STOP mutation on the dipeptide affinities of ^{VP}HNP (Table 1) and of des 1−6^{VP}BNP (*9*).

What do these data have to do with the pathogenicity of the 87STOP mutant? We suggest that the predicted instability of the monomeric state of both proteins at physiological pH and temperature, and at a redox potential comparable to that in the ER, points to the absence of copeptin as a primary contributor to mutant pathogenicity. This instability predicts that a significant fraction of monomers will initially misfold—and accordingly depend on chaperone and disulfide isomerase interactions for refolding—while awaiting a stabilizing folded partner subunit. Given that the WT full-length precursor (HVP) does not have the in vivo folding problems of the 87STOP mutant, and that NP residues 87−93 do not make a significant net thermodynamic contribution to stability, these considerations indicate that, in vivo, either CP (which is glycosylated in vivo*)* thermodynamically stabilizes the monomeric state of HVP or that it or residues 87−93 play roles in chaperone interaction. A dependence of chaperone interaction on residues 87−93 seems unlikely. This sequence is not strictly conserved, particularly when both oxytocin and VP precursors are considered (e.g., ref *27*), and, in any case, chaperones of the Hsp70 class such as BiP do not have a significant sequence specificity (*32*). This leaves a role only for copeptin.

The above argument is in part based on negative data. We also acknowledge that the conditions of our studies are nonidentical to ER conditions, although it is difficult to predict the effects of these differences. Protein crowding effects in the ER, for example, have been shown to increase folding in some cases, and aggregation in others (e.g., ref *33*). Nonetheless, we point to strong evidence from in vivo studies, which has recently come to our attention, indicating a role for glycosylated copeptin in the folding of the rat VP precursor. Specifically, earlier immunohistochemical studies of normal adult rats and other mammals (*34*, *35*) demonstrated the accumulation of filamentous "accretions" of the oxytocin precursor in the ER of oxytocinergic neurons,. VP precursor accretions were not found in VP-synthesizing neurons (*34*), but were shown in the rat to be induced in these neurons by tunicamycin-induced inhibition of glycosylation (*36*); levels of tunicamycin eliciting this induction had no effect on oxytocin neurons, indicating inhibition of copeptin glycosylation, given the absence of any other glycosylation site in either precursor (*36*). These results relate significantly to our present data and hypotheses. Assuming that the accretions represent misfolded protein, the results

indicate that misfolded WT oxytocin precursor accumulates with time in the ER of oxytocin-synthesizing neurons, but that quantities are insufficient to kill these neurons. This is consistent with the demonstration here of the greater stability of the bovine oxytocin precursor than of either HVPΔCP or the pathogenic 87STOP mutant,[3] as evidenced by its lesser susceptibility to guanidine denaturation and the less oxidizing environment required for its folding (Methods). However, the presence of these accretions only in oxytocinergic neurons also means that the oxytocin precursor, which does not contain copeptin and which is more stable than HVPΔCP, folds in vivo less efficiently than the full-length VP precursor, which contains copeptin. This points to a role for copeptin. Most importantly, the results argue that glycosylation (and therefore copeptin) is important to the normal intraneuronal handling of the wild-type rat VP precursor. By extension, the lack of copeptin in the 87STOP mutant would be expected to contribute to its pathogenicity.

What role does glycosylated copeptin play? We found no evidence for stabilization by unglycosylated CP, but cannot exclude such stabilization by glycosylated CP. However, a more likely role is interaction with the calnexin/calreticulin system (*37*, *38*). This system monitors protein folding and interacts principally (but perhaps not exclusively) with the sugars of glycosylated proteins, bringing these proteins into the proximity of a glycoprotein-specific member of the protein disulfide isomerase family. Significantly, efficient folding of human lipopotein lipase, a glycosylated disulfide-containing dimeric enzyme, has recently been shown to depend on calreticulin, which decreases the formation of inactive monomers and increases formation of active dimers (*39*), a situation potentially reflecting thermodynamic instability of the monomeric state as proposed here for the VP precursor. While arguments have been raised against any role for copeptin in the VP precursor (introduction), our results and consideration of the properties of the calnexin/calreticulin system indicate that the arguments are not irrefutable, i.e., the absence of CP in the oxytocin precursor is explainable by the greater stability of this precursor, and the cell culture results are subject to alternative interpretations. Specifically, because the calnexin/calreticulin system is known to significantly decrease the rate of protein folding, while increasing its efficiency (e.g., ref *37*), the increase in VP secretion in cell culture accompanying deletion of copeptin from the rat VP precursor (*14*) actually suggests release from control by the calnexin/calreticulin system. Moreover, because the cell culture studies measured only VP secretion (*13*, *14*), a decrease in folding efficiency could well be masked by a larger increase in folding rate. Such an explanation is particularly attractive because it removes the apparent contradiction between the cell culture and intraneuronal studies of the rat precursor.

The above interpretation does not exclude a role for other factors in mutant pathogenicity. For example, the solubility of misfolded states of the 87STOP mutant potentially augments pathogenicity via the same mechanism proposed above for its effects on in vitro folding.[4] The decreased dimerization constant of the mutant might also decrease the rate at which monomers are stabilized by dimerization. Such possibilities remain to be explored. However, the preponderance of evidence indicates that the primary source of the folding defect in the 87STOP mutant is the instability of its folded monomeric state and the loss, resulting from copeptin deletion, of thermodynamic or (more probably) biological mechanisms to compensate for this instability. Such a situation is analogous, albeit not identical, to that recently reported (*40*) in which a quantitatively comparable instability of mutants of superoxide dismutase, solely in their apo states accounts, for their pathogenicity. These and related results (e.g., ref *39*) call attention to the importance of the frequently unknown mechanisms by which such unstable initial products of folding (monomers in the case of dimers and higher oligomers, apo states in the case of metalloproteins) are prevented from denaturation and aggregation prior to maturation to their biologically active forms, and the consequent role of these mechanisms in modulating disease processes.

ACKNOWLEDGMENT

The authors express their appreciation to Tam L. Nguyen and Mandar Naik for the NMR spectroscopy, to Fatemah Mamdani for constructive comments, to Min Lu of this department for the ultracentrifuge studies, and to Art Villafania for excellent technical assistance in the early phase of these studies.

APPENDIX

Analysis of pH-Induced Dissociation of Intramolecular Hormone−NP Interactions. The concentrations of all internally liganded and unliganded components at the midpoint of the dissociation curves in Figure 6 were constrained using dimerization constants for unliganded ^{VP}HNP and ^{VP}HNP87STOP of 2.3×10^3 and 8×10^2 M^{-1}, respectively (Table 1). The choice of these values is based on the assumption that any deprotonation of precursor Lys and Tyr at the titration midpoint (pH 9.5) does not affect dimerization, as for example justified by the failure of amino group succinylation (*9*), or an increase in pH from 8 to 10 (unpublished observations), to affect ^{Oxy}BNP dimerization; the Lys and Tyr residues of ^{Oxy}BNP are identical to those of ^{VP}HNP (Figure 1). Interactions between two liganded monomers and between one liganded and unliganded monomer were assigned equilibrium constants 100-fold higher and 10-fold higher, respectively, than that of the corresponding unliganded protein, the thermodynamic parallel of a 10-fold higher binding constant to a dimer subunit than to a monomer. From the derived concentrations, the internal hormone−NP association constants were calculated, with

[3] The greater stability of the oxytocin precursor than the VP precursor is unlikely to be restricted to a comparison of the bovine oxytocin precursor with the human VP precursor. Our stability studies to date of different NP derivatives (e.g., refs *9*, *20*, and this paper) can be shown to suggest that the differences between ^{Oxy}BNP and both ^{VP}HNP and ^{VP}BNP (e.g., Tables 1 and 3) reflect their differences in the sequence 75−86. While the overall identity between oxytocin-related and VP-related NPs is approximately 70%, this sequence is unique in having only 25% identity when the two series are compared, while exhibiting strong intraseries identities when different species are compared (e.g., ref *27*). Moreoever, relative to ^{Oxy}BNP, the substitutions seen at β-sheet residues 80 and 81 in the oxytocin series (*27*) were shown to strongly stabilize porcine ^{Oxy}NP (*20*) and tend towards increased β-sheet propensity in the other cases.

[4] Although the pathogenicity of HVPΔCP is unknown, the extreme insolubility of its misfolded states might also contribute to pathogenicity by preventing their clearance.

results accepted when agreement between the calculated values and these constraints was within 10%. Several corrections were then necessary to convert the initially derived monomer and dimer binding constants to their concentration-independent values at pH 7.4 and 37 °C. First, it can be shown that the intramolecular binding constant determined at 0.05 M concentration (1585) contains a contribution from the uphill free energy necessary to increase the total dimer content from its value in the completely unliganded state to that at the titration midpoint. The total dimer content calculated at the titration midpoint relative to that calculated in the absence of binding gave the energy correction (calculated as 0.5[Δ mole fraction dimer] *RT*ln [dimer concentration at titration midpoint/dimer concentration in unliganded state]). Correction for this energy term increased the originally derived binding constants by 26%. Values were corrected to 37 °C by decreasing the 25 °C binding constant of the protonated hormone α-amino group by 50% based on literature data (e.g., ref *21*) and on unpublished studies in this laboratory. Binding constants were corrected to pH 7.4 to account for amino group deprotonation in the unbound state using a pK_a value of 6.0 at 37 °C to adjust for temperature effects on pK_a.

Effects of Concentration on NP Stability. Concentration effects on NP stability to guanidine denaturation arise because of the free energy ($-\Delta G_{\text{Dimerization}}$) required to dissociate the equilibrium population of folded unliganded NP dimer to folded unliganded monomers during the unfolding process, where

$$\Delta G_{\text{Dimerization}} = \Delta G^{\circ}_{\text{Unliganded dimerization}} + RT\ln \frac{(\text{Dimer})_{\text{equilibrium}}}{(\text{Monomer})^2_{\text{initial}}} \quad (3)$$

and the initial concentration of monomer is the total molar concentration of NP chains. The stabilities of unliganded NP monomers and dimers (0.1 M) to guanidine denaturation at pH 7.4 were calculated from measured stabilities of unliganded NP to guanidine denaturation at 0.05 mM, pH 6 (Table 1) as described in the Table 4 legend. Standard free energies of dimerization were calculated from the measured dimerization constants in Table 1 of ^{VP}HNP at pH 6.2 and 7.5 and of ^{VP}HNP87STOP at pH 6.2, using the assumption that dimerization of ^{VP}HNP87STOP, like that of ^{VP}BNP, is unchanged between pH 6.2 and 7.5 because of the absence of His-90. Stabilities were assumed to be unchanged between 25 and 37 °C.

REFERENCES

1. Rittig, S., Robertson, G. L., Siggaard, C., Kovacs, L., Gregersen, N., Nyborg, J., and Pedersen, E. B. (1996) Identification of 13 new mutations in the vasopressin-neurophysin II gene in 17 kindred with familial autosomal dominant neurohypophyseal diabetes insipidus, *Am. J. Hum. Genet. 58*, 107−117.
2. Ito, M., Jameson, L., and Ito, M. (1997) Molecular Basis of Autosomal Dominant Neurohypophyseal Diabetes Insipidus. Cellular Toxicity Caused by the Accumulation of Mutant Vasopressin Precursors within the Endoplasmic Reticulum, *J. Clin. Invest. 99*, 1897−1905.
3. Nijenhuis, M., Zalm, R., and Burbach, J. P, (2000) A diabetes insipidus vasopressin prohormone altered outside the central core of neurophysin accumulates in the endoplasmic reticulum, *Mol. Cell Endocrinol. 167*, 55−67.
4. Beuret, N., Rutishauser, J., Bider, M. D., and Spiess, M. (1999) Mechanism of Endoplasmic Reticulum Retention of Mutant Vasopressin Precursor Caused by a Signal Peptide Truncation Associated with Diabetes Insipidus, *J. Biol. Chem. 274*, 18965−18972.
5. Rutishauser, J., Kopp, P., Gaskill, M. B., Kotlar, T. J., and Robertson, G. L. (2002) Clinical Study: Clinical and molecular analysis of three families with autosomal dominant neurohypophyseal diabetes insipidus associated with a novel and recurrent mutations in the vasopressin-neurophysin II (AVP-NP II) gene, *Eur. J. Endocrinol. 146*, 649−656.
6. Land, H., Schutz, G., Schmale, H., and Richter, D. (1982) Nucleotide sequence of cloned cDNA encoding bovine arginine vasopressin-neurophysin II precursor, *Nature 295*, 299−303.
7. Rittig, S., Siggaard, C., Ozata, M., Yetkin, I., Gregersen, N., Pedersen, E. B., and Robertson, G. L. (2002) Autosomal Dominant Neurohypophyseal Diabetes Insipidus due to Substitution of Histidine for Tyrosine$_2$ in the Vasopressin Moiety of the Hormone Precursor, *J. Clin. Endocrinol. Metab. 87*, 3351−3355.
8. Land, H., Grez, M., Ruppert, S., Schmale, H., Rehbein, M., Richter, D., and Schutz, G. (1983) Deduced amino acid sequence from the bovine oxytocin-neurophysin I precursor cDNA, *Nature 302*, 342−344.
9. Eubanks, S., Nguyen, T. L., Deeb, R., Villafania, A., Alfadhli, A., and Breslow, E. (2001) Effects of Diabetes Insipidus Mutations on Neurophysin Folding and Function, *J. Biol. Chem. 276*, 29671−29680.
10. Wu, C. K., Hu, B., Rose, J. P., Liu, Z.-J, Nguyen, T. L., Zheng, C., Breslow, E., and Wang, B.-C. (2001) Structures of an unliganded neurophysin and its vasopressin complex: Implications for binding and allosteric mechanisms, *Protein Sci. 10*, 1869−1880.
11. Fassina, G., and Chaiken, I. M. (1989) Sequence simplification and the intra- and intermolecular self-recognition properties of vasopressin/neurophysin biosynthetic precursor, *J. Mol. Recognit. 1*, 158−165.
12. Rabbani, D., Pagnozzi, M., Chang, P., and Breslow, E. (1982) Partial digestion of neurophysins with proteolytic enzymes: unusual interactions between bovine neurophysin II and chymotrypsin, *Biochemistry 21*, 817−826.
13. Iwasaki, Y., Oiso, Y., Saito, H., and Majzoub, J. S. (2000) Effects of various mutations in the neurophysin/glycopeptide portion of the vasopressin gene on vasopressin expression in vitro, *Tohoku J. Exp. Med. 191*, 187−202.
14. Kim, J. K., Summer, S. N., Wood, W. M., Brown, J. L., and Schrier, R. W. (1997) Arginine vasopressin secretion with mutants of wild-type and Brattleboro rats AVP gene, *J. Am. Soc. Nephrol. 8*, 1863−1869.
15. Eubanks, S., Lu, M., Peyton, D., and Breslow, E. (1999) Expression, Folding, and Thermodynamic Properties of the Bovine Oxytocin-Neurophysin Precursor: Relationships to the Intermolecular Oxytocin-Neurophysin Complex, *Biochemistry 38*, 13530−13541.
16. Kaiser, R., and Metzka, L. (1999) Enhancement of cyanogen bromide cleavage yields for methionyl-serine and methionyl-threonine peptide bonds, *Anal. Biochem. 266*, 1−8.
17. Huang, H.-b., and Breslow, E. (1992) Identification of the unstable neurophysin disulfide and localization to the hormone-binding site. Relationship to folding-unfolding pathways, *J. Biol. Chem. 267*, 6750−6756.
18. Deeb, R., and Breslow, E. (1996) Thermodynamic Role of the Pro Region of the Neurophysin Precursor in Neurophysin Folding: Evidence from the Effects of Ligand Peptides on Folding, *Biochemistry 35*, 864−873.
19. Zheng, C., Peyton, D., and Breslow, E. (1997) Modulation of dimerization by residues distant fron the interface in bovine neurophysin-II, *J. Peptide Res. 50*, 199−209.
20. Eubanks, S., Nguyen, T., Peyton, D., and Breslow, E. (2000) Modulation of Dimerization, Binding, Stability, and Folding by Mutation of the Neurophysin Subunit Interface, *Biochemistry 39*, 8085−8094.
21. Nicolas, P., Batelier, G., Rholam, M., and Cohen, P. (1980) Bovine neurophysin dimerization and neurohypophyseal hormone binding, *Biochemistry 19*, 3565−3573.
22. Breslow, E., LaBorde, T., Bamezai, S., and Scarlata, S. (1991) Binding and fluorescence studies of the relationship between neurophysin-peptide interaction and neurophysin self-associa-

tion: an allosteric system exhibiting minimal cooperativity, *Biochemistry 30*, 7990−8000.
23. Samuel, D., Kuman, T. K., Ganesh, G., Jayaraman, G., Yang, P. W., Chang, M. M., Trivedi, V. D., Wang, S. L., Hwang, K. C., Chang, D. K., and Yu, C. (2000) Proline inhibits aggregation during protein refolding**,** *Protein Sci. 9*, 344−52.
24. Breslow, E., Weis, J., and Menendez-Botet, C. J. (1973) Small peptides as analogues of oxytocin and vasopressin in their interactions with bovine neurophysin-II, *Biochemistry 12*, 4644−4653.
25. Ando, S., McPhie, P., and Chaiken, I. M. (1987) Sequence redesign and the assembly mechanism of the oxytocin/bovine neurophysin I biosynthetic precursor, *J. Biol. Chem. 262*, 12962−12969.
26. Pace, C. N. (1975) The stability of globular proteins, *Crit. Rev. Biochem. 3*, 1−43.
27. Chauvet, M. T., Hurpet, D., Chauvet, J., and Acher, R. (1983) Identification of Human Neurophysins: Complete Amino Acid Sequences of MSEL-and VLDV-Neurophysins, *Proc. Natl. Acad. Sci. U.S.A. 80*, 2839−2843.
28. Kanmera, T., and Chaiken, I. M. (1985) Molecular properties of the oxytocin/bovine neurophysin biosynthetic precursor. Studies using a semisynthetic precursor, *J. Biol. Chem. 260*, 8474−8482.
29. Dreifuss, J. J. (1975) A review on neurosecretory granules: their contents and mechanisms of release, *Ann. N. Y. Acad. Sci. 248*, 184−199.
30. Oprins, A., Rabouille, C., Posthuma, G., Klumperman, J., Geuze, H. J., and Slot, J. W. (2001) The ER to Golgi interface is the major concentration site of secretory proteins in the exocrine pancreatic cell, *Traffic 2*, 831−838.
31. Hwang, C., Sinskey, A. J., and Lodish, H. F. (1992) Oxidized redox state of glutathione in the endoplasmic reticulum, *Science 22*, 1496−1502.
32. Misselwitz, B., Staeck, O., and Rapoport, T. A. (1998) J proteins catalytically activate Hsp70 molecules to trap a wide range of peptide sequences, *Mol. Cell 2*, 593−603.
33. van den Berg, B., Ellis, R. J., and Dobson, C. M. (1999) Effects of macromolecular crowding on protein folding and aggregation, *EMBO J. 18*, 6927−6933.
34. Pow, D. V., Morris, J. F., and Rodgers, S. (1991) Peptide accretions in the endoplasmic reticulum of magnocellular neurosecretory neurons in normal and experimentally manipulated rats, *J. Anat. 178*, 155−174.
35. Pow, D. V. (1992) Peptide accretions in the endoplasmic reticulum of oxytocinergic neurons in cats, monkeys and rabbits: a widespread phenomenon, *J. Anat. 181*, 161−167.
36. Pow, D. V., and Morris, J. F. (1992) Tunicamycin, puromycin and brefeldin A influence the subcellular distribution of neuropoeptides in hypothalamic magnocellular neurons of rat, *Cell Tissue Res. 269*, 547−560.
37. Parodi, A. J. (2000) Protein glucosylation and its role in protein folding, *Annu. Rev. Biochem. 69*, 69−93.
38. Schrag, J. D., Procopio, D. O., Cygler, M., Thomas, D. Y., and Bergeron, J. J. (2003) Lectin control of protein folding and sorting in the secretory pathway, *Trends Biochem. Sci. 28*, 49−57.
39. Zhang, L., Wu, G., Tate, C. G., Lookene, A., and Olivecrona, G. (2003) Calreticulin promotes folding/dimerization of human lipoprotein lipase expressed in insect cells (Sf21), *J. Biol. Chem. 278*, 29344−29351.
40. Lindberg, M. J., Tibell, L., and Oliveberg, M. (2002) Common denominator of Cu/Zn superoxide dismutase mutants associated with amyotrophic lateral sclerosis: Decreased stability of the apo state, *Proc. Natl. Acad. Sci. U.S.A.* 24, 16607−16612.
41. Burbach, J. P. H., and de Bree, F. M. (1998**)** Structure−function relationships of the vasopressin prohormone domains, *Cell Mol. Neurobiol. 18*, 173−191.
42. Ausubel, F. M., Brent, R., Kingston, R. E., Moore, D. D., Seidman, J. G., Smith, J. A., and Struehl, K., Eds., *Current Protocols in Molecular Biology*, Wiley, New York.

BI0400094